Theor Chem Acc (2010) 126:257–263
DOI 10.1007/s00214-009-0700-3

REGULAR ARTICLE

Electron localizability and polarizability in tight-binding graphene nanostructures

Stefano Evangelisti · Gian Luigi Bendazzoli · Antonio Monari

Received: 17 October 2009 / Accepted: 11 November 2009 / Published online: 1 December 2009
© Springer-Verlag 2009

Abstract Graphene nanostructures are analyzed in the framework of the modern theory of conductivity (Resta in J Chem Phys 124:104104, 2006), and the metallic character of the systems is analyzed and discussed. The electronic wavefunction is studied by using a tight-binding approximation. In particular, we focus our attention on nanostructures having hexagonal shapes and D_{2h} symmetry. Band structure, specific (i.e., per-atom) polarizability and localizability (or localization tensor) have been numerically computed for several structures. The different behavior of the three parameters, is analyzed, as well as their usefulness in assesing the metal character of a system. A special emphasis is devoted to the discussion of the rather surprising behavior of the specific polarizability.

Keywords Graphene · Nano-structures · Polarizability · Modern theory of conductivity

1 Introduction

The peculiar behavior of the localizability and polarizability tensors of graphene nanostructures is presented in this work. Graphene nanoislands are composed of hexagonal unities of sp^2-hybridized carbon atoms. These structures can be considered as finite portions, extracted from a formally infinite graphene sheet. Therefore, while sharing some important characteristics of the bidimensional graphene, they also experience some remarkable difference, in particular due to the emergence of edge and bord effects [1–4]. Recent experiments have shown that nanometer-sized graphene islands (or flakes) can be produced on various surfaces [5–11]. This has of course induced a significant amount of theoretical interest [12–23] on the peculiar behavior of those structures. We remind that in the real systems, the peripheral carbons are saturated by hydrogen atoms. Obviously, in the case of a tight-binding approximation, the hydrogen atoms do not have any influence on the π Hamiltonian.

In this work, in particular, we focus our attention on structures having, broadly speaking, a "hexagonal" shape and D_{2h} symmetry (some examples are shown in Figs. 1, 2, 3). We remind that all the structures studied in the present paper present so called "zigzag" edges. The investigated structures, lying on the xy plane, are uniquely characterized by two integer numbers: the length N and the width M. The length is equal to the maximum number of adjacent hexagons in the x direction. The width is given by the maximum number of adjacent zigzag hexagons in the y direction.

Some values of N and M have been particularly investigated:

- The value $M = 1$ gives the polyacene series (Fig. 1, top).
- The general case $M < N$ gives zigzag hexagonal graphene nanoribbons (Fig. 1, bottom).
- For $M = N = 3$, one gets the coronene molecule. Therefore, more generally, the $M = N$ sequence will be called the coronene series (see Fig. 2).
- Finally, the case $N = 2$, $M = 3$ gives the pyrene molecule, and the sequence $M = 2N - 1$ gives the pyrene series (Fig. 3).

Dedicated to the memory of Professor Jean-Pierre Daudey and published as part of the Daudey Memorial Issue.

S. Evangelisti · A. Monari
Laboratoire de Chimie et Physique Quantiques, UMR 5626, Université de Toulouse et CNRS, 118, Route de Narbonne, 31062 Toulouse Cedex, France

G. L. Bendazzoli · A. Monari (✉)
Dipartimento di Chimica Fisica e Inorganica, Università di Bologna, Viale Risorgimento 4, 40136 Bologna, Italy
e-mail: amonari@ms.fci.unibo.it; antonio.monari@irsamc.ups-tlse.fr

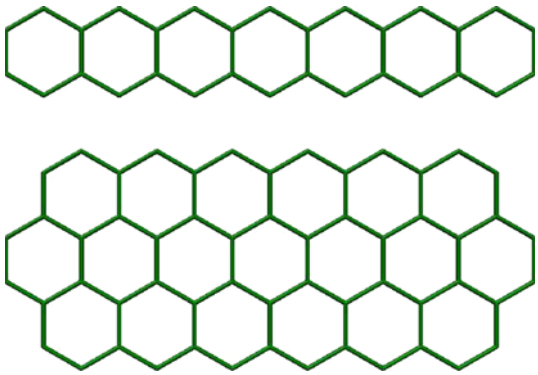

Fig. 1 The molecular structure for the (7,1) (*top*) and (7,3) (*bottom*) nanoribbons

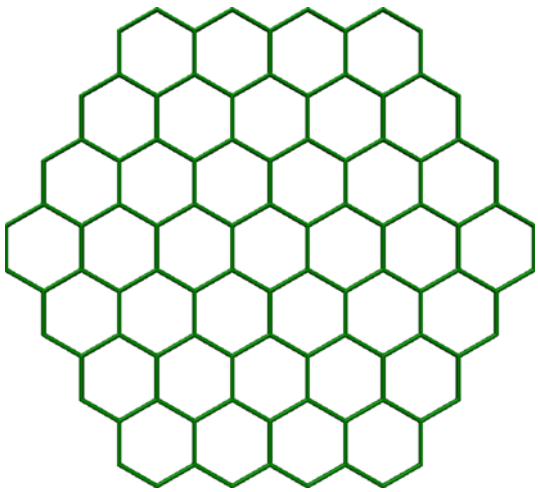

Fig. 2 The molecular structure for the (7,7) hypercoronene

Notice that M cannot be larger than $2N - 1$. Since we are mainly interested in the behavior of polarizability and localizability, i.e., the main parameters involved in the modern theory of conductivity, we report here a brief summary of the key concepts of this formalism. Modern theory of conductivity emerged in a well-defined manner following the pioneer works of Kohn in the 1960s [24]. Different authors contributed to its development in the recent years [25–30] and the real key parameter involved in such definition is the so called localization tensor as defined by Resta [26, 29]. Although this theory was originally developed in the framework of periodic boundary conditions, its extension in the case of finite non-periodic clusters is clearly more appropriate for the present investigation [29]. We indicate by $|\Psi\rangle$ an electronic wavefunction, by $\hat{\mathbf{r}}_i$, the position operator of the ith electron (the position operator being a vector quantity of Cartesian

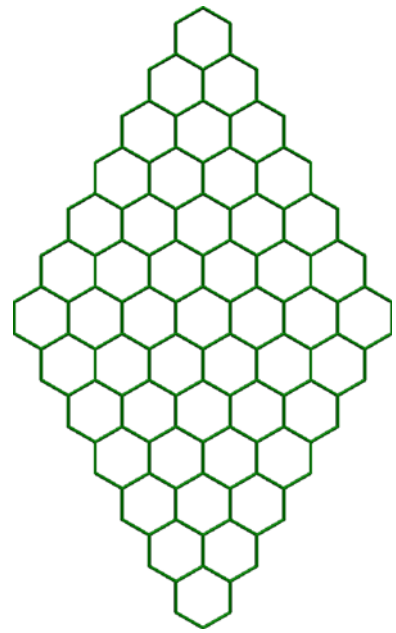

Fig. 3 The molecular structure for the (7,13) hyperpyrene

components x, y, z), and by $\hat{\mathbf{r}}_\beta$ one Cartesian component of the total position operator

$$\hat{\mathbf{r}} = \sum_{i=1}^{n} \mathbf{r}_i \tag{1}$$

One can then define the cumulant of the second order momentum with respect of the operator $\hat{\mathbf{r}}$ (quadratic fluctuation of the position)

$$\langle r_\beta r_\gamma \rangle_c = \frac{1}{n}\left(\langle \Psi|\hat{r}_\beta \hat{r}_\gamma|\Psi\rangle - \langle \Psi|\hat{r}_\beta|\Psi\rangle\langle \Psi|\hat{r}_\gamma|\Psi\rangle\right) \tag{2}$$

Notice that the $\frac{1}{n}$ factor has been introduced to eliminate the dependence on n in the case of identical *non-interacting* subsystems. In the following, for the sake of simplicity of notation, the locality-tensor components $\langle r_\beta r_\gamma \rangle_c$ will be simply indicated as $\rho_{\beta\gamma}$ and the definition of localizability will be used in analogy with polarizability. An equivalent, and in some cases more convenient, expression of the localizability can be obtained through the spectral-resolution form as:

$$\begin{aligned}\langle r_\beta r_\gamma \rangle_c &= \langle \Psi_0|(r_\beta - \langle r_\beta \rangle)|(r_\gamma - \langle r_\gamma \rangle)|\Psi_0\rangle \\ &= \sum_{k>0} \langle \Psi_0|r_\beta|\Psi_k\rangle\langle \Psi_k|r_\gamma|\Psi_0\rangle\end{aligned} \tag{3}$$

Here the vectors $|\Psi_k\rangle$ are the (excited) eigenvectors of the system while $|\Psi_0\rangle$ represents the ground state. The relation between localizability and polarizability is strongly enhanced when the two quantities are expressed in the spectral-resolution form, the (static) polarizability being expressed as:

$$\alpha_{\beta\gamma} = 2\sum_{k>0}\left(\frac{\langle\Psi_0|r_\beta|\Psi_k\rangle\langle\Psi_k|r_\gamma|\Psi_0\rangle}{E_k - E_0}\right) \quad (4)$$

where E_k are the eigenvalues corresponding to the Ψ_k eigenvector, E_0 being the ground state energy. As shown in [29] in the case of a metallic system the localizability tensor will diverge, while for insulators it will converge to a finite value. It is also important to remind that the localizability tensor has been formally related to the conductivity of a system by Souza and Wilkinson [30] in a fundamental paper. Recently, this formalism has been applied to the study of the metal–insulator transition both at ab initio level [31] and by using a Hückel Hamiltonian [32]. According to these works, the metallic character of a system can be investigated by using three different criteria:

1. Zero energy gap.
2. Infinite per-atom polarizability.
3. Infinite fluctuation of the position operator (localizability).

Anyway, it has to be pointed out that while the energy gap relates the metallic behavior of a system only to the states close to the Fermi level, the polarizability and the localizability are able to take into account the properties of the whole system as it is clear from the spectral-resolution formalism. Moreover, the localizability being defined as the quadratic spread of the electronic position, this parameter is also able to account for the delocalization of states which is needed for metallic character to emerge.

It is also important to remind that strictly speaking, since we are dealing with finite systems, it is impossible to obtain a true metallic behavior. However, the divergent or convergent behavior of the localizability (and of the per-atom polarizability) is a clearly evidenced, and therefore one can reasonably speak of a sort of metallicity, or at least of the presence of "precursors" of metallic characters.

In this paper we study the polarizability, localizability and band structure (or the density of states) of graphene nanostructures at tight-binding level (i.e., by using a Hückel-type Hamiltonian) as a function of N and M. The polarizability being an extensive quantity, in contrast with localizability (see Eq. 3), in the following we will always refer to the specific (or per-atom) polarizability. It turns out that these quantities present sometimes a rather surprising behavior. In the case of polyacenes, for instance, the specific transversal-specific polarizability becomes larger than the longitudinal one for N sufficiently large. In the case of long ribbons, the transversal-specific polarizability diverges, while the longitudinal one tends to a finite limit. The corresponding localizabilities, on the other hand, remain finite even in the limit of infinite system. In the case of the hyperpyrene series, both components of specific polarizability and localizability tensors diverge, although following a different behavior (polynomial vs. exponential).

It would be interesting to investigate whether these results are associated with this extremely simplified one-electron Hamiltonian, or if they can be found by using more complex, and possibly ab initio, formalisms. This aspect will be treated in a forthcoming paper. Undoubtedly, the observed behavior can be related to the appearance of edge states [1] on the graphene nanostructures, an occurrence that has been confirmed at ab initio level for instance by Scuseria et al. [2, 3]. In any case, our results show that the three conditions that are often seen as the signature of metallic behavior (diverging specific polarizability and localizability, zero gap) are not equivalent each other.

2 Computational details

All the investigated nanostructures have a D_{2h} symmetry. As discussed in the Sect. 1, they are uniquely characterized by two integer numbers: the length N and the width M. In this study, both N and M have been chosen to be *odd* integer numbers. Three special cases, polyacenes ($M = 1$), hypercoronenes ($M = N$), and hyperpyrenes ($M = 2N - 1$), have been particularly investigated. Notice that, in hexagonal structures, M cannot be larger than $2N - 1$.

Due to the one-electron nature of the Hückel Hamiltonian, numerically "exact" solutions can be obtained in the case of fairly large values of N and M. Only the carbon p orbitals that are perpendicular to the symmetry plane have been considered and a very simple Tight-Binding (TB), or Hückel, Hamiltonian, based on the atom connectivity, has been used. Only interactions between first neighboring atoms have been retained and set equivalent to β (sometimes also called the hopping integral t). Notice that, because of the loss of the linear geometry, the Hückel Hamiltonian is no more tridiagonal, and therefore, the computational cost considerably increases. If one works in the molecular-orbital (MO) basis obtained by a diagonalization of the Hamiltonian, the ground-state wavefunction is described by a single determinant, obtained by filling the MO's via the aufbau principle.

Since the position is a one-electron operator, the sum over states, involved both in the polarizability and locality calculation becomes a sum over single excitations, which, if N is even, are in number of $(N/2)^2$ for each value of the spin projection. The same computational cost is required to compute the polarizability and the locality tensors if the sum over state formalism is assumed. Hence, because of this simple structure of the wavefunction, the computational cost of the locality and polarizability grows only as N^3 in the case of large N. In this way, it was possible to treat systems composed of up to 10^3 centers. All the

calculations were performed by using the BLAS routines (http://www.netlib.org/blas/).

Finally, molecular orbital densities reported in the following have been obtained by using the Molekel visualization software. Orbital densities have been obtained from the Hückel eigenvectors (molecular orbitals) placing a symmetric gaussian function on each carbon atoms (atomic orbitals) with an arbitry exponential coefficient. For this reason, only one lobe is visible in the represented orbitals, the other one being hidden by the orbitals themselves.

3 Results and discussion

We discuss first the longitudinal (ρ_x and α_x with our convention) and transversal (ρ_y and α_y) components of the localizability and specific polarizability in narrow hexagonal structures. Both the transversal and longitudinal localizabilities of narrow structures have very weak dependendence on the structure length. On the other hand, the *transversal*-specific polarizability strongly depends on the ribbon *length*. In Figs. 4 and 5, the longitudinal and transversal values of ρ and α are reported as a function of N for the first three narrow ribbon, $M = 1$, $M = 3$, and $M = 5$. For large values of N, the transversal specific polarizability α_y grows as N^M.

The corresponding localizabilities ρ_y do not show any divergent behavior for large N. These numerical results seem to indicate that divergent specific polarizability and localizability are not, in fact, equivalent criteria in order to judge about the metallicity of a material. One should note, moreover, that the energy gap of these systems is vanishing. This fact would suggest a "metallic" behavior (in agreement with the specific polarizability results), although it is difficult to discuss about conductivity in the y direction, since the system has a fixed narrow extension in this direction.

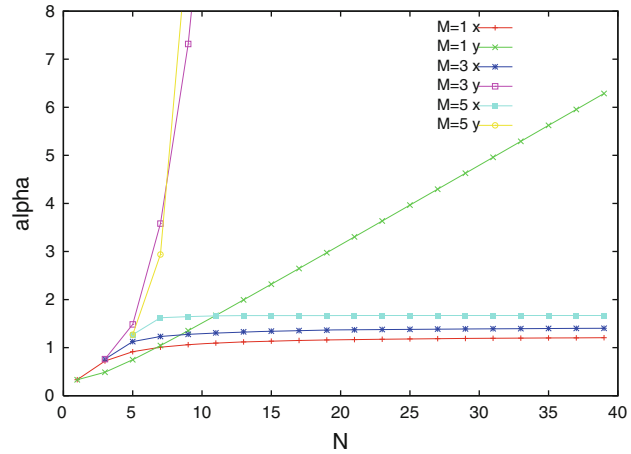

Fig. 5 Longitudinal (α_x) and transversal (α_y) specific polarizabilities of the (N, M) chains as a function of N, for the three different values of M ($M = 1, 3, 5$)

If both N and M are increased, one obtains truly two-dimensional systems. In Fig. 6, the localizabilities of (N, N) structures (hypercoronenes) and (N, N) (hyperpyrenes) are shown. All localizabilities (ρ_x and ρ_y for pyrenes, and ρ_{xy} for coronenes) have a linear growth as a function of N. This is in accord with a similar behavior of linear Hückel chains [32]. Specific polarizabilities (Fig. 7), on the other hand exhibit a less systematic trend, although they show a divergent growth in the case of both structures (see Tables 1 and 2). The y component of pyrene-specific polarizability grows exponentially. The coronene degenerated specific polarizabilities also grow exponentially, but with a much smaller exponential factor. Finally, the x component of pyrene specific polarizability has a slow linear behavior.

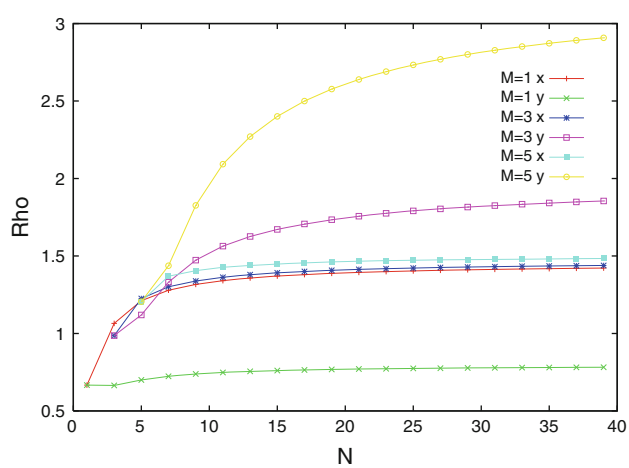

Fig. 4 Longitudinal (ρ_x) and transversal (ρ_y) localizabilities of the (N, M) chains as a function of N, for the three different values of M ($M = 1, 3, 5$)

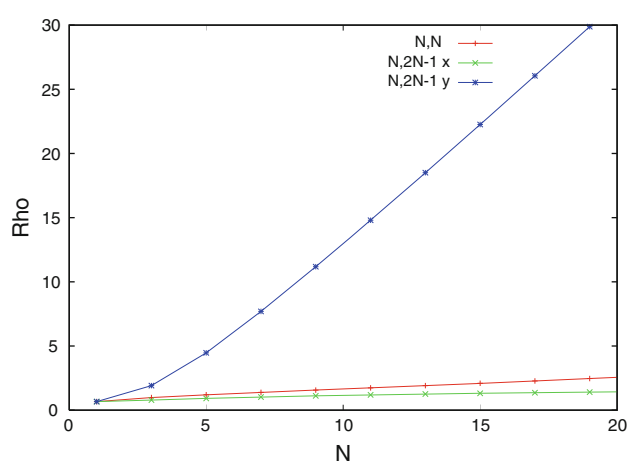

Fig. 6 Localizabilities: $\rho_{xy}(N, N)$ for the coronene series, and $\rho_x(N, 2N - 1)$ and $\rho_y(N, 2N - 1)$ for the pyrene series

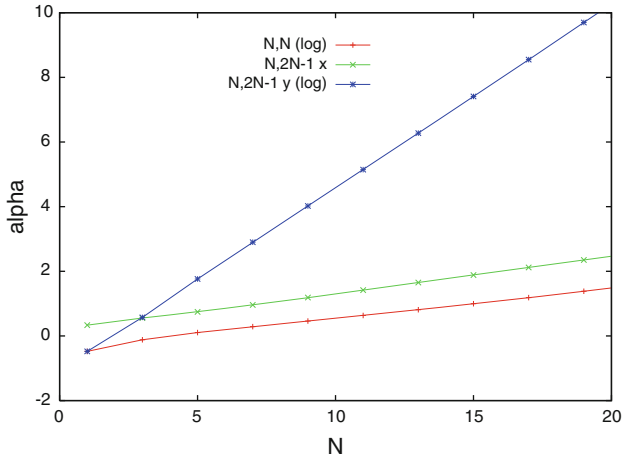

Fig. 7 Specific polarizabilities: $\alpha_{x=y}(N, N)$ for the coronene series, and $\alpha_x(N, 2N-1)$ and $\alpha_y(N, 2N-1)$ for the pyrene series. Notice that $\alpha_{x=y}(N, N)$ and $\alpha_y(N, 2N-1)$ are reported in logarithmic scale, while $\alpha_x(N, 2N-1)$ is linear

Table 1 Localizabilities (a.u) of two nanoisland species: the (N, N) series (hypercoronenes) and the $(N, 2N-1)$ series (hyperpyrenes)

N	$\rho_{x,y}(N, N)$	$\rho_x(N, 2N-1)$	$\rho_y(N, 2N-1)$
1	0.6667	0.6667	0.6667
3	0.9863	0.7914	1.9135
5	1.2052	0.9145	4.4655
7	1.3900	1.0246	7.6931
9	1.5638	1.1160	11.1795
11	1.7366	1.1924	14.7997
13	1.9125	1.2576	18.5016
15	2.0926	1.3143	22.2582
17	2.2765	1.3643	26.0536
19	2.4635	1.4091	29.8777
21	2.6526	1.4496	33.7237

The two values ρ_x and ρ_x are degenerated in the case of the (N, N) series, and are noted as $\rho_{x,y}$. In d^2 (where d is formally the nearest neighbor distance)

In Figs. 8 and 9, the localizabilities and specific polarizabilities of generic (N, M) structures is illustrated. In particular, the $(N, 19)$ and the $(N, 39)$ cases are shown as a function of N. Both ρ and α show a non-monotonic behavior, although the figure scales are different (linear for ρ, logarithmic for α. The x components show a slow growth, up to a maximum which corresponds to the hypercoronene structure, (N, N). Then the quantity slowly decreases. The y components grow very quickly, they pass for a maximum close to $M = N/2$, and then reach a sharp *minimum* for hypercoronenes. Then they start growing again, up to very large values. Notice that transversal and longitudinal components of the localizability and polarizability tensors have to be degenerate in the case of hypercoronenes ($M = N$) due to symmetry reasons. It should be stressed that extremely similar behaviors are shown by localizabilities in linear scale and specific polarizabilities in logarithmic scale.

Table 2 Specific polarizabilities (a.u) of two nanoisland species: the (N, N) series (hypercoronenes) and the $(N, 2N-1)$ series (hyperpyrenes). The two values α_x and α_y are degenerated in the case of the (N, N) series, and are noted as $\alpha_{x,y}$

N	$\alpha_{x,y}(N, N)$	$\alpha_x(N, 2N-1)$	$\alpha_y(N, 2N-1)$
1	0.3333	0.3333	0.3333
3	0.7616	0.5547	3.7458
5	1.2703	0.7431	57.8434
7	1.9411	0.9594	793.5145
9	2.8931	1.1875	10497.2950
11	4.3109	1.4188	139479.9983
13	6.4915	1.6514	1878936.5142
15	9.9184	1.8843	25681494.5339
17	15.3839	2.1175	355704447.2941
19	24.1900	2.3507	4984478082.3343
21	38.4786	2.5841	70559376761.8645

In $\frac{d^2}{\beta}$ (where d is formally the nearest neighbor distance)

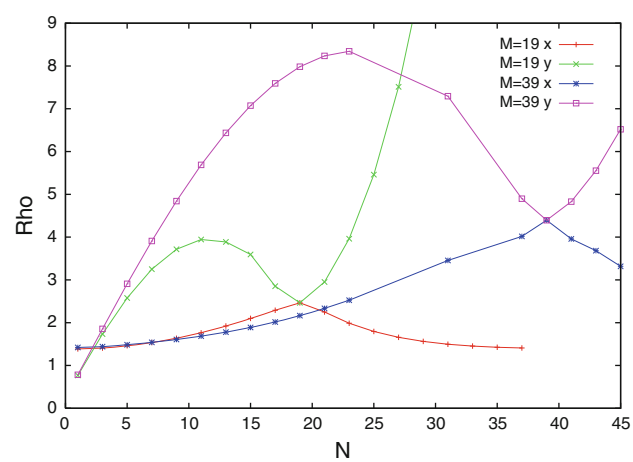

Fig. 8 Longitudinal $\rho_x$and transversal ρ_y localizability for the $(N, 19)$ and $(N, 39)$ nanoislands as a function of N

Figure 10 illustrates the band structure of two different nanoislands: the (39,39) hypercoronene, and the (39,77) hyperpyrene. They are representative of the behavior of the two families. The energy bands of the two systems are extremely close, and the curves are hardly distinguishable at the figure scale. On the other hand, if the Fermi-level region is blown up (see Fig. 11), some important differences appear. These differences can explain the strongly different behavior of static polarizabilities and localizabilities of the two series, as pointed out previously. In particular, the hyperpyrene energy levels tend exponentially to the Fermi energy, while hypercoronene experiences a much slower behavior. Therefore, one can

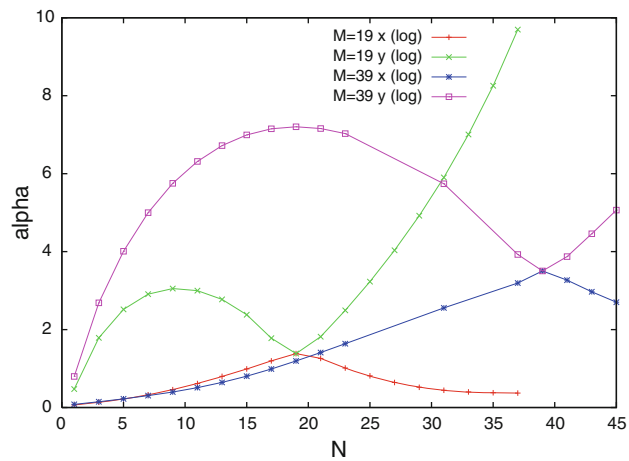

Fig. 9 Longitudinal $\alpha_x$and transversal α_y specific polarizability for the (N, 19) and (N, 39) nanoislands as a function of N. In logarithmic scale

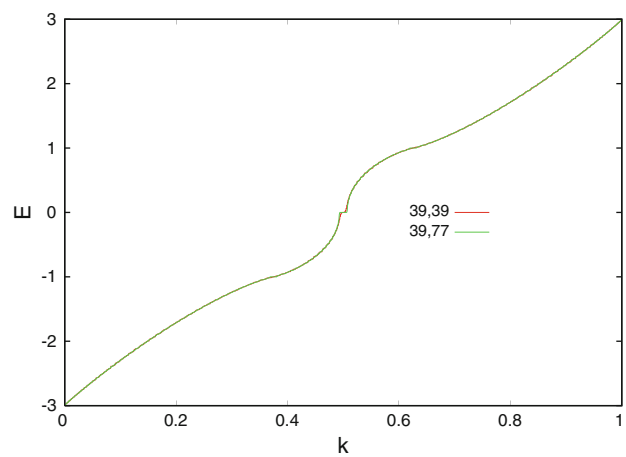

Fig. 10 Orbital energies (β units) of the (39,77) hyperpyrene as a function of k. A single band is assumed

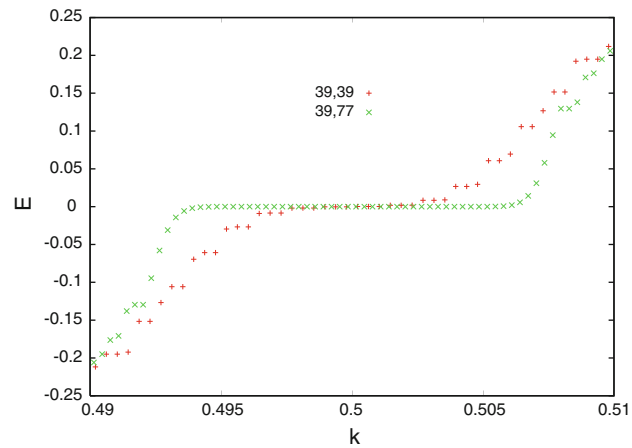

Fig. 11 Zoom of the orbital energies of the (39,77) hyperpyrene as a function of k

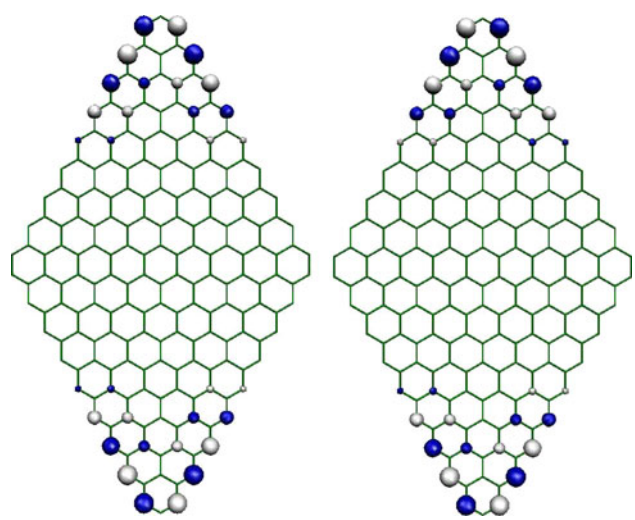

Fig. 12 HOMO (*left*) and LUMO (*right*). Orbital densities of the (9,17) hyperpyrene

underline a different behavior of the energy levels near the Fermi level: an exponentially decreasing gap for hyperpyrenes, and a polynomial one for hypercoronenes. This fact explains why, although the band structure of both (N, N) hypercoronenes and (N, $2N - 1$) hyperpyrenes tend to the band structure of graphene in the bulk limit (large N values), the localizabilities and specific polarizabilities of these systems diverge in a completely different way.

Finally, in Fig. 12, the electronic densities for the highest occupied molecular orbital (HOMO) and the lowest unoccupied molecular orbital (LUMO) have been reported for the (9,17) hyperpyrene. One can immediately see how frontier orbitals tend to concentrate at the edge of the systems, therefore confirming the significative presence of edge effects. Moreover HOMO orbital is symmetric along the vertical (y) direction while LUMO is antisymmetric; therefore, the combination of the two with the dipole moment operator y leads to a non-vanishing quantity. Because the two orbitals are essentially degenerate this fact can explain the fast diverging of the α_y specific polarizability, since the denominator in the sum over states formalism (see Eq. 4) will rapidly tend to zero. On the other hand, on the longitudinal x direction the two orbitals are symmetric; therefore, both numerator and denominator in the sum over states expression will be vanishing. A similar interpretation can be invoked for the longitudinal divergent behavior in the (N, M) nanoribbons.

4 Conclusions

The present tight-binding study on graphene nanostructures (nanoislands) points out some, rather unexpected, noteworthy results:

- In the case of narrow structures having a fixed width M, the longitudinal-specific polarizability and both components of localizability remain small.
- For the same clusters, the transversal-specific polarizability grows as N^M. Therefore, the transversal-specific polarizability becomes much larger than the longitudinal one, even for relatively small structures.
- In the case of more compact structures (hypercoronenes, hyperpyrenes), we assist to a similar behavior.
- Two-dimensional structures exhibit a diverging density of states at the Fermi level. The precise form of the energy band, on the other hand, depends strongly on the geometrical shape of the nanoislands.

These results imply that the diverging of the localizability and specific polarizability tensors are non-equivalent indicators, as was also observed in the case of the dimerization of linear chains [32]. The divergence of the localizability tensor seems more suitable to be associated to the metal character of a system, since localizability measuring the quadratic dispersion of the electron positions is directly related to electronic state delocalization. Therefore, in this regard, the infinite polyacene seems to behave like an insulator rather than a metal in the orthogonal direction. It should be noted, however, that for these systems the HOMO–LUMO gap is zero in the limit of an infinite length.

The present results are limited, at the moment, to the use of a TB Hamiltonian; the use of more complex ab initio Hamiltonians will be addressed in further studies.

Acknowledgments This article is dedicated to the memory of Jean-Pierre Daudey, to whom one of us (S.E.) was bound by a long-lasting scientific and personal friendship. This work was partly supported by the French "Centre National de la Recherche Scientifique" (CNRS, also under the PICS action 4263), and the Italian Ministry of University and Research (MUR). Support from the European Community within the COST program [the COST D37 (GRIDCHEM) and COST CM0702 actions] is also gratefully acknowledged.

References

1. Davidson SG, Stęślicka M (1992) Basic theory of surface states, Clarendon, Oxford
2. Hod O et al (2007) Phys Rev B 76:233401
3. Hod O et al (2008) Phys Rev B 77:035411
4. Son Y-W et al (2006) Nature (London) 444:347
5. Berger C et al (2004) J Phys Chem 108:19912
6. Novoselov KS, Geim AK, Morozov SV, Jiang D, Zhang Y, Dubonos SV, Grigorieva IV, Firsov AA (2004) Science 306:666
7. Novoselov KS, Geim AK, Morozov SV, Jiang D, Katsnelson MI, Grigorieva IV, Dubonos SV, Firsov AA (2005) Nature 438:197
8. Berger C et al (2006) Science 312:1191
9. Novoselov KS, Jiang Z, Zhang Y, Morozov SV, Stormer HL, Zeitler U, Maan JC, Boebinger GS, Kim P, Geim AK (2007) Science 315:1379
10. Geim AK, Novoselov KS (2007) Nat Mater 6:183
11. Li G, Andrei EA (2007) Nat Phys 3:623
12. Alicea J, Fisher MPA (2005) Phys Rev B 74:75422
13. Gusynin VP, Sharapov SG (2005) Phys Rev Lett 95:146801
14. Tworzydlo J, Trauzettel B, Titov M, Rycerz A, Beenakker CWJ (2006) Phys Rev Lett 96:246802
15. Gusynin VP, Sharapov SG, Carbotte JP (2006) Phys Rev Lett 96:256802
16. Zhou SY, Gweon GH, Graf J, Fedorov AV, Spataru CD, Diehl RD, Kopelevich Y, Lee DH, Louie SG, Lanzara A (2006) Nat Phys 2:595
17. Yamamoto T, Noguchi T, Watanabe K (2006) Phys Rev B 74:121409
18. Nomura K, MacDonald AH (2007) Phys Rev Lett 98:76602
19. Son YW, Cohen ML, Louie SG (2007) Phys Rev Lett 97:216803
20. Areshkin DA, Gunlycke D, White CT (2007) Nano Lett 7:204
21. Chen J-H, Jang C, Xiao S, Ishigami M, Fuhrer MS (2008) Nat Nanotechnol 3:206
22. Castro EV, Peres NMR, Lobes dos Santos JMB, Castro Neto AH, Guinea F (2008) Phys Rev Lett 100:026802
23. Akhmerov AR, Beenakker CWJ (2008) Phys Rev B 77:085423
24. Kohn W (1964) Phys Rev 133:A171
25. Resta R (1998) Phys Rev Lett 80:1800
26. Resta R, Sorella (1999) Phys Rev Lett 82:370
27. Aoki Y, Imamura A (1995) J Chem Phys 103:9726
28. Resta R (2005) Phys Rev Lett 95:196805
29. Resta R (2006) J Chem Phys 124:104104
30. Souza I, Wilkens T, Martin RM (2000) Phys Rev B 62:1666
31. Vetere V, Monari A, Bendazzoli GL, Evangelisti S, Paulus B (2008) J Chem Phys 128:024701
32. Monari A, Bendazzoli G L, Evangelisti S (2008) J Chem Phys 129:134104